



ORIGINAL ARTICLE

Synthesis, antifungal activity and *in vitro* mechanism of novel 1-substituted-5-trifluoromethyl-1*H*-pyrazole-4-carboxamide derivatives



Jingxin Yang, Dewen Xie, Chengzhi Zhang, Cailong Zhao, Zhibing Wu*, Wei Xue*

State Key Laboratory Breeding Base of Green Pesticide and Agricultural Bioengineering, Key Laboratory of Green Pesticide and Agricultural Bioengineering, Ministry of Education, Center for R&D of Fine Chemicals of Guizhou University, Guiyang 550025, China

Received 27 February 2022; accepted 19 May 2022
Available online 21 May 2022

KEYWORDS

Pyrazole carboxamides;
Molecular design;
Fungicidal activity;
Molecular docking;
SAR analysis;
Antifungal mechanism

Abstract Inspired by the wide application of amides in plant pathogens, a series of novel 1-substituted-5-trifluoromethyl 1*H* pyrazole-4-carboxamide derivatives were designed and synthesized. Bioassay results indicated that some target compounds exhibited excellent and broad-spectrum *in vitro* and certain *in vivo* antifungal activities. Among them, the *in vitro* EC₅₀ values of **Y₁₃** against *G. zae*, *B. dothidea*, *F. proliferatum* and *F. oxysporum* were 13.1, 14.4, 13.3 and 21.4 mg/L, respectively. The *in vivo* protective activity of **Y₁₃** against *G. zae* at 100 mg/L was 50.65%. SAR analysis revealed that the phenyl on the 1-position of the pyrazole ring was important for this activity. An antifungal mechanism study of **Y₁₃** against *G. zae* demonstrated that this compound may disrupt the cell membrane of mycelium, thus inhibiting the growth of fungi. These mechanistic study results were inconsistent with those for traditional amides and may provide a novel view for deep study of this series of pyrazole carboxamide derivatives.

© 2022 The Authors. Published by Elsevier B.V. on behalf of King Saud University. This is an open access article under the CC BY-NC-ND license (<http://creativecommons.org/licenses/by-nc-nd/4.0/>).

1. Introduction

Plant diseases reduce the global production of major food and economic crops by 20% per year (Xiong et al., 2013). Phy-

topathogenic fungi cause a drastic threat to agricultural development and human health (McColl et al., 2018). The consequences of plant diseases caused by pathogenic fungi can be catastrophic (Wang et al., 2014). Some fungi can produce mycotoxins, which pose a significant threat for human and animal health (Ninomiya et al., 2020). Currently, chemical means are still the main method to prevent and control fungal diseases (Al-Otibi et al., 2021). Due to the frequent use of commercialized fungicides, pathogenic fungi have evolved severe resistance (Oporto et al., 2019). Therefore, it is necessary to develop novel structural skeletons with clear targets or molecules with novel mechanisms (Wang et al., 2021).

* Corresponding authors.

E-mail addresses: zbwu@gzu.edu.cn (Z. Wu), wxue@gzu.edu.cn (W. Xue).

Peer review under responsibility of King Saud University.



Amides are basic molecular structures that have been widely studied and applied and from which a series of commercial fungicides have been derived. They exhibit wide biological activities, including insecticidal (Luo et al., 2020), herbicidal (Wang et al., 2019), antifungal (Yang et al., 2019) and anticancer activities (Chen et al., 2020). Analysis of the commercially available amide fungicides revealed that many of them use a pyrazole amide as the active skeleton. Among the structures of pyrazole-4-carboxamides, there are two typical types of substitutions on the pyrazole ring: 1,3-disubstitution and 1,3,5-trisubstitution (Fig. 1) (Abrigach et al., 2016; Hua et al., 2020; Xiong et al., 2017; Zhang et al., 2017; Liu et al., 2019; Zhang et al., 2019; Du et al., 2018; Yan et al., 2019; Liu et al., 2018; Gonzalez-Lopez et al., 2020).

In previous work, we found an active skeleton of 5-trifluoromethyl-4-pyrazole carboxamide, and its derivatives exhibited excellent inhibitory activity against *Fusarium oxysporum* as potential succinate dehydrogenase inhibitors (Wu et al., 2021). In the present study, the 5-trifluoromethyl on the pyrazole ring of the active skeleton was preserved, the phenyl on the 1-position of the pyrazole ring was substituted by a series of alkyl and cyclohexyl groups, and a series of novel 1-substituted-5-trifluoromethyl-4-pyrazole carboxamide derivatives were designed and synthesized. Bioassay evaluation and docking analysis were used to determine the necessity of the phenyl on the pyrazole ring. The antifungal mechanism of active compounds against *Gibberella zeae* (Schwein.) Petch was also investigated.

2. Methods and materials

2.1. Instruments and chemicals

^1H NMR, ^{13}C NMR, and ^{19}F NMR spectra were obtained on a JEOL-500 (JEOL CO., Ltd., Japan) or a Bruker 400 NMR

spectrometer (Bruker Corporation, Germany) with tetramethylsilane as an internal standard and CDCl_3 or $\text{DMSO}-d_6$ as the solvent. HRMS data were acquired on a Thermo Scientific Q Exactive mass spectrometer (Thermo Scientific, USA). The morphology of the fungus was observed using an Olympus BX53 fluorescence microscope (Olympus Ltd, Japan) and a Nova Nano SEM 450 instrument (FEI Company, USA). The MDA contents were recorded on a Cytation 5 imaging reader (BioTek Instruments, USA). The MDA assay kit was purchased from Beijing Solarbio Science & Technology Co., and all reagents and solvents were of analytical grade.

2.2. Fungi

Seven plant pathogenic fungi were used for antifungal evaluation. *Thanatephorus cucumeris*, *Diaporthe phaseolorum* var. *phaseolorum* (Cooke & Ellis) Sacc, *Gibberella zeae* (Schwein.) Petch, *Fusarium oxysporum*, and *Fusarium oxysporum* f. sp. *Cucumerinum* were purchased from Beijing Beina Chuanglian Biotechnology Institute, China. *Fusarium proliferatum* was isolated and identified in our lab from Guizhou University, and *Botryosphaeria dothidea* was provided by Guiyang University. These fungi were grown on PDA plates at $25 \pm 1^\circ\text{C}$ and maintained at 4°C .

2.3. Synthesis

2.3.1. General procedure for the synthesis of 3a-3e

In a round-bottom flask, ethyl trifluoroacetate (0.1 mol), triethyl orthoformate (0.2 mol) and acetic anhydride (0.3 mol) were mixed, stirred at 130°C for 4 h, and then subjected to vacuum distillation to obtain **2**. Cyclohexyl hydrazine hydrochloride (3.45 g, 22.90 mmol) was dissolved in ethanol (50 mL); the pH value was adjusted to 7 with sodium hydroxide solution; and then, **2** was added and reacted at 100°C for 2 h. The solvent was removed by vacuum distillation. The mix-

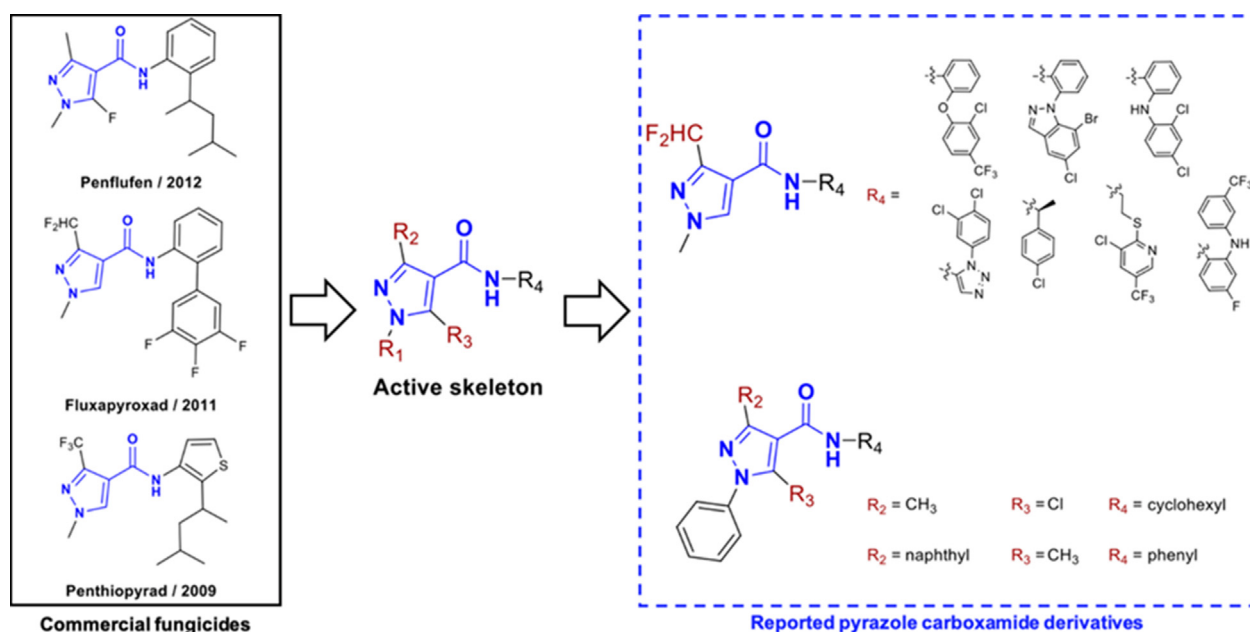


Fig. 1 Representative fungicides containing pyrazole carboxamide moieties.

ture was extracted with ethyl acetate, washed with brine, dried over anhydrous sodium sulfate and concentrated to obtain the crude product. The crude product was further purified by column chromatography (PE/EA = 50/1) to obtain **3c**. The physical and spectral data of **3a-3e** are provided in the [Supporting Information](#).

2.3.2. General procedure for the synthesis of **4a-4e**

Intermediate **3c** (6.0 g, 20.7 mmol), THF (30 mL), and water (30 mL) were added in turn. After the solution was uniformly stirred, lithium hydroxide (2.0 g, 82.7 mmol) was added. The reaction mixture was stirred for 2 h at 80 °C. The solution was concentrated in vacuo. Hydrochloric acid (2 M) was used to adjust the pH value to approximately 4; some solid precipitates formed, and the mixture was filtered. The filtrate was washed with water and dried to obtain **4c**. The physical and spectral data of **4a-4e** are provided in the [supporting information](#).

2.3.3. General procedure for the synthesis of **5a-5e**

According to a method reported in the literature ([Komane et al., 2020](#)), using SOCl₂ as the solvent, **5a-5e** were synthesized. The solvent was removed under vacuum after the reaction was finished, and the crude product was directly used for the next reaction.

2.3.4. General procedure for the synthesis of **Y₁-Y₂₀**

Taking **Y₉** as an example, a solution of 4-aminopyridine (3.2 mmol), intermediates **5c** (3.5 mmol) and NaH (6.4 mmol) in anhydrous THF (5 mL) was stirred at room temperature overnight. The residue was extracted with ethyl acetate and water, dried over anhydrous sodium sulfate, and purified by silica gel column chromatography to obtain **Y₉**. The physical and spectral data of target compounds **Y₁-Y₂₀** are provided in the [supporting information](#).

2.4. Bioassays

2.4.1. *In vitro* antifungal activity

According to a previously reported method ([Jian et al., 2016](#)), the fungicidal activities of target compounds **Y₁-Y₂₀** were tested against seven pathogenic fungi. The preliminary activity screening concentration of the compounds was 100 mg/L. DMSO (1%) in sterile distilled water served as a blank control, whereas the commercial fungicides boscalid, penthiopyrad, fluopyram and phenamacril served as the positive controls. Compounds with high inhibition rates were measured at the EC₅₀ value. Inhibitory effects were calculated as follows: inhibition efficiency (%) = $[(L_0 - L)/(L_0 - 0.5)] \times 100$, where L₀ represents the diameter of fungal growth in the blank control and L represents the diameter of the fungi treated with compound. Each condition was performed in triplicate. SD values were calculated based on the inhibition data for triplicates of each inhibition rate. The regression equations and R² values are provided in the [Supporting Information](#).

2.4.2. *In vivo* protective activity bioassay

Maize seeds (Zhengdan 958) were planted in moist soil and cultured in a constant temperature incubator at 25 °C until germination. Seedlings with the same growth and health were

transplanted into pots and cultivated for 4 d. A solution of **Y₁₃** (100 mg/L) and phenamacril (100 mg/L) was sprayed on the leaves. DMSO (1%) was used as a blank control. After two days in the incubator, the corn leaves were polished with sandpaper, and then, mycelia were placed on the wounds and moisturized with wet cotton. Lesion length was measured after 10 d. The control efficacies were calculated as follows: control efficacy (%) = $(A_0 - A_1)/A_0 \times 100$, where A₀ represents the length of the lesion in the blank control group and A₁ represents the length of the lesion treated with compound. SD values were calculated based on the inhibition data for triplicates of each inhibition rate ([Wang et al., 2021](#)).

2.5. Molecular docking

The SDH crystal structures were downloaded from the RCSB PDB database (PDB codes: 2FBW, 3AEG and 7D6V) and used for the docking study. All bound water and key ligands were eliminated from SDH. Six compounds (**Y₁**, **Y₅**, **Y₉**, **Y₁₃**, fluopyram and penthiopyrad) were selected as the docking ligands, and energies of ligands were minimized using MM2 energy minimizations in ChemBio 3D ([Fu et al., 2021](#)). Software of Sybyl X 2.1 was used for molecular docking, and the ligands were embedded well in the same protein activity pocket (established by the extraction carboxin or boscalid from SDH or established automatically) ([Kim et al., 2009](#); [Kim et al., 2009](#)). Surflex-Dock method was used to simulate and evaluate the interactions between the ligands and the target protein using an empirical scoring function in Surflex-Dock Geom (SFXC) mode ([Kaddouri et al., 2020](#); [Wang et al., 2020](#); [Kaddouri et al., 2021](#)).

2.6. Antifungal mechanism study

2.6.1. Mycelial quantity after treatment of *G. Zeae* with **Y₁₃**

Mycelia of *G. zeae* were cultured on PDB medium on a rotary shaker at 25 °C and 180 rpm. Then, solutions of **Y₁₃** at different concentrations (0 mg/L, 6.25 mg/L, 12.5 mg/L, 25 mg/L, 50 mg/L, 100 mg/L and 200 mg/L) were added and incubated with the mycelia for 24 h at 25 °C. Mycelial samples were filtered out of the medium and dried by vacuum freezing. The weighing was repeated three times, each reading difference did not exceed 0.01 g, and each dry mycelium weight is reported as the average dry mycelium weight ([Zhu et al., 2020](#)).

2.6.2. Cell membrane integrity study

Morphological observation of hyphae via FM: Mycelia of *G. zeae* were cultured on PDB medium on a rotary shaker at 25 °C and 180 rpm. Then, solutions of **Y₁₃**, penthiopyrad and phenamacril at different concentrations (0 mg/L, 50 mg/L, 100 mg/L and 200 mg/L, respectively) were added and incubated with the mycelia for 24 h at 25 °C. The PDB medium was removed by centrifugation at 4 °C and 3381 g for 5 min, and the hyphae were stained with 10 μL of a PI solution (20 mg/L). The hyphae were incubated at 37 °C for 15 min in the dark and then washed with PBS three times. A coverslip was placed on the hyphae, and the samples were observed and photographed using an Olympus-BX53 fluorescence microscope ([Hou et al., 2021](#)).

Morphological observation of hyphae via SEM: Mycelia of *G. zeae* were cultured on PDB medium on a rotary shaker

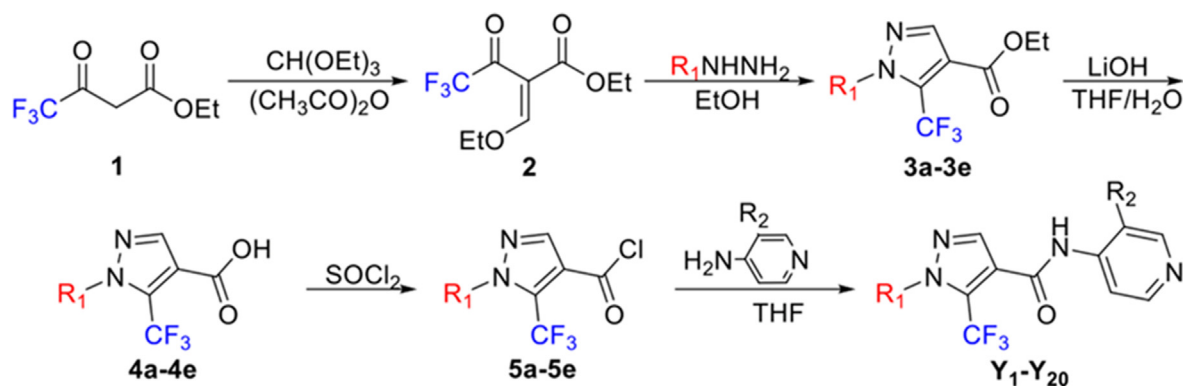


Fig. 2 Synthesis routes of the target compounds Y_1 - Y_{20} .

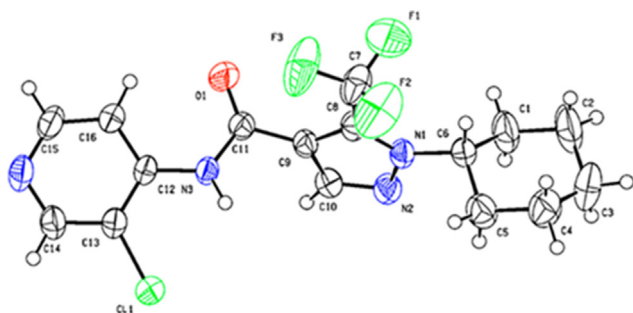


Fig. 3 Crystal structure of Y_{11} .

(180 rpm) at 25 °C and 180 rpm. Then, prepared solutions of Y_{13} , penthiopyrad and phenamacril at different concentrations (0 mg/L and 200 mg/L, respectively) were added and incubated with the mycelia for 24 h at 25 °C. The mycelia were then washed three times with PBS solution, and 2.5% glutaraldehyde solution was added for fixation for 24 h. The mycelia were washed with 30%, 50%, 70%, 90%, 100% ethanol and 100% *tert*-butanol, dried in a freeze-dryer, sprayed with gold, made into samples and observed (Ke et al., 2022).

2.6.3. Determination of MDA contents

Mycelia of *G. zea* were cultured on PDB medium on a rotary shaker (180 rpm) at 25 °C and 180 rpm. Then, prepared solu-

Table 1 Inhibition effect of target compounds against seven plant phytopathogenic fungi at 100 mg/L. ^a.

Compound no.	R_1	R_2	Inhibition rate \pm SD (%)						
			<i>GZ</i>	<i>TC</i>	<i>BD</i>	<i>DP</i>	<i>FP</i>	<i>FOC</i>	<i>FO</i>
Y_1	methyl	H	0	11.0 \pm 3.0	0	31.2 \pm 1.2	0	–	8.6 \pm 0.6
Y_2	methyl	CH ₃	0	0	0	0	0	–	9.4 \pm 2.3
Y_3	methyl	Cl	12.8 \pm 1.6	29.4 \pm 1.5	0	21.8 \pm 0.6	10.5 \pm 2.2	–	15.7 \pm 1.1
Y_4	methyl	F	0	0	17.2 \pm 2.1	17.5 \pm 0.9	0	–	13.5 \pm 0.0
Y_5	isopropyl	H	40.9 \pm 0.5	0	9.6 \pm 0.7	34.0 \pm 1.8	32.8 \pm 1.1	–	23.9 \pm 0.6
Y_6	isopropyl	CH ₃	15.0 \pm 1.4	13.7 \pm 2.5	36.8 \pm 2.5	0	63.2 \pm 1.0	–	49.5 \pm 1.1
Y_7	isopropyl	Cl	64.7 \pm 1.3	40.8 \pm 1.0	68.9 \pm 2.1	32.0 \pm 0.6	81.8 \pm 2.3	66.8 \pm 1.8	60.0 \pm 2.0
Y_8	isopropyl	F	41.9 \pm 1.6	53.1 \pm 0.8	47.4 \pm 0.4	78.9 \pm 2.0	76.2 \pm 0.6	47.8 \pm 0.2	55.4 \pm 1.1
Y_9	cyclohexyl	H	77.2 \pm 1.1	75.7 \pm 0.4	69.2 \pm 1.7	20.3 \pm 9.6	65.6 \pm 0.6	55.7 \pm 1.2	63.6 \pm 3.0
Y_{10}	cyclohexyl	CH ₃	23.4 \pm 1.1	51.4 \pm 0.3	31.8 \pm 1.2	0	23.5 \pm 0.6	–	22.6 \pm 2.3
Y_{11}	cyclohexyl	Cl	0	20.2 \pm 1.6	15.9 \pm 1.4	0	0	–	0
Y_{12}	cyclohexyl	F	27.8 \pm 3.2	37.7 \pm 3.0	28.5 \pm 1.3	0	30.5 \pm 1.7	–	31.8 \pm 0.1
Y_{13}	<i>o</i> -methylphenyl	H	86.6 \pm 0.2	68.2 \pm 1.4	86.1 \pm 0.6	100	61.8 \pm 0.7	92.3 \pm 0.3	70.8 \pm 0.9
Y_{14}	<i>o</i> -methylphenyl	CH ₃	67.6 \pm 0.4	84.3 \pm 0.0	79.7 \pm 0.4	100	55.0 \pm 0.7	67.2 \pm 0.6	63.3 \pm 0.6
Y_{15}	<i>o</i> -methylphenyl	Cl	45.4 \pm 3.2	62.0 \pm 1.4	33.6 \pm 3.1	52.2 \pm 3.2	42.0 \pm 0.0	21.8 \pm 1.3	50.6 \pm 1.1
Y_{16}	<i>o</i> -methylphenyl	F	68.0 \pm 1.1	77.6 \pm 3.1	73.9 \pm 0.3	83.7 \pm 0.7	39.1 \pm 0.7	59.0 \pm 4.0	53.2 \pm 1.7
Y_{17}	<i>o</i> -trifluorophenyl	H	83.7 \pm 1.5	54.1 \pm 1.3	76.4 \pm 0.4	89.8 \pm 0.9	81.5 \pm 1.5	81.2 \pm 0.8	79.8 \pm 0.0
Y_{18}	<i>o</i> -trifluorophenyl	CH ₃	62.1 \pm 1.5	64.3 \pm 3.0	74.8 \pm 1.9	94.3 \pm 1.4	41.2 \pm 1.9	59.0 \pm 0.5	45.3 \pm 0.6
Y_{19}	<i>o</i> -trifluorophenyl	Cl	0	24.7 \pm 0.7	19.7 \pm 5.2	40.0 \pm 0.7	0	–	0
Y_{20}	<i>o</i> -trifluorophenyl	F	37.3 \pm 2.0	29.4 \pm 0.6	57.3 \pm 0.2	51.4 \pm 0.7	24.4 \pm 1.3	–	46.8 \pm 1.7
boscalid			16.3 \pm 0.6	100	28.5 \pm 1.5	39.6 \pm 1.4	0	–	12.4 \pm 1.1
penthiopyrad			0	100	–	–	–	–	–
fluopyram			72.5 \pm 0.6	–	–	–	–	–	–
phenamacril			100	–	–	–	–	–	–

^a Values are the means \pm SD of three replicates. ‘–’, not tested.

GZ: *Gibberella zea* (Schwein.) Petch; *TC*: *Thanatephorus cucumeris*; *BD*: *Botryosphaeria dothidea*; *DP*: *Diaporthe phaseolorum* var. *phaseolorum* (Cooke & Ellis) Sacc; *FP*: *Fusarium proliferatum*; *FOC*: *Fusarium oxysporum* f. sp. *Cucumerinum*; *FO*: *Fusarium oxysporum*.

Table 2 EC₅₀ values of certain target compounds against seven types of plant phytopathogenic fungi. ^a

Compound no.	EC ₅₀ (mg/L)						
	GZ	TC	BD	DP	FP	FOC	FO
Y ₁₃	13.1 ± 2.7	49.8 ± 5.7	14.4 ± 0.6	36.4 ± 0.4	13.3 ± 1.4	38.9 ± 1.1	21.4 ± 0.6
Y ₁₄	50.7 ± 1.7	37.5 ± 2.4	18.1 ± 3.9	26.6 ± 3.9	–	–	26.0 ± 1.1
Y ₁₆	56.0 ± 0.8	44.3 ± 1.4	20.6 ± 0.3	21.8 ± 3.0	34.3 ± 1.7	112.3 ± 1.7	–
Y ₁₇	16.8 ± 0.4	56.8 ± 0.9	13.9 ± 0.6	–	–	–	37.8 ± 2.0
Y ₁₈	–	94.6 ± 16.7	–	–	–	–	–
fluopyram	12.3 ± 0.3	–	–	–	–	–	–
penthiopyrad	–	0.1 ± 0.0	–	–	–	–	–
boscalid	–	3.5 ± 0.1	–	–	–	–	–
phenamacril	0.5 ± 0.0	–	–	–	–	–	–

^a Values are the means ± SD of three replicates. '–', not tested.

GZ: *Gibberella zeae* (Schwein.) Petch; TC: *Thanatephorus cucumeris*; BD: *Botryosphaeria dothidea*; DP: *Diaporthe phaseolorum* var. *phaseolorum* (Cooke & Ellis) Sacc; FP: *Fusarium proliferatum*; FOC: *Fusarium oxysporum* f. sp. *Cucumerinum*; FO: *Fusarium oxysporum*.

Table 3 In vivo protective activity of Y₁₃ against *G. zeae* at 100 mg/L.

Compound no.	Protective activity	
	diameter of lesions (cm)	control efficacy (%)
CK	3.0 ± 1.0 ^a	–
Y ₁₃	1.4 ± 0.4 ^b	50.65 ± 3.3
phenamacril	0.6 ± 0.1 ^c	79.83 ± 4.8

^{a b c} The significant difference analysis adopts Duncan's test method, and IBM SPSS Statistics 20 data processing software was used. Different letters in the same column in the table indicate significant differences, *p* < 0.05.

tions of compound Y₁₃ at different concentrations (0 mg/L, 25 mg/L, 50 mg/L, 100 mg/L, and 200 mg/L) were added and incubated with the mycelia for 24 h at 25 °C. The medium was filtered out, and the hyphae were collected in a vacuum freeze dryer. Mycelia (0.1 g) were homogenized in an ice bath with 1 mL of MDA extract (produced by Solarbio Technology Co., Ltd., Beijing, China) and centrifuged at 8000 g and 4 °C for 15 min. The supernatant was removed, added to each reagent according to the kit instructions, held in a 100 °C water bath for 60 min, cooled in an ice bath, and centrifuged at 10,000 g for 10 min at room temperature. The supernatant was aspirated, and then, the absorbance of each sample was measured at 450 nm, 532 nm and 600 nm. Each group was repeated three times. MDA content in mycelia was determined using an MDA assay kit (Beijing Solarbio Science & Technology Co.) (Mo et al., 2021).

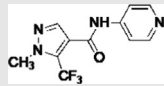
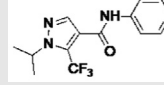
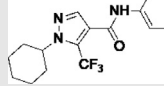
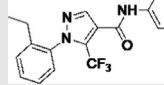
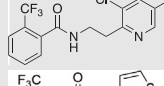
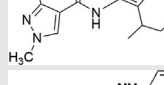
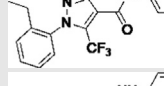
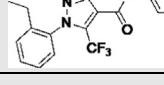
3. Results and discussion

3.1. Chemistry

3.1.1. Synthesis

The synthetic route of 1-substituted-5-trifluoromethyl-1H-pyrazole-4-carboxamide derivatives is shown in Fig. 2. Intermediate **2** was obtained by condensing **1** and triethyl orthoformate and then cyclized with different hydrazines to obtain intermediates **3a-3e**. Intermediates **4a-4e** were synthesized through a hydroxide reaction of **3a-3e** in the presence of lithium hydrox-

Table 4 Total docking score between ligands and SDH proteins.

PDB code	Ligand	Structure	Total score
	Y ₁		4.3
	Y ₅		3.5
	Y ₉		5.4
2FBW	Y ₁₃		6.3
	fluopyram		7.1
	penthiopyrad		7.3
3AEG	Y ₁₃		6.2
7D6V	Y ₁₃		6.2

ide. The acylation products **5a-5e** were obtained by electrophilic substitution reaction of **4a-4e** with SOCl₂ and reacted with substituted 4-pyridine amines to yield the target compounds Y₁-Y₂₀. All the target compounds were confirmed by ¹H NMR, ¹³C NMR, and ¹⁹F NMR spectroscopy and HRMS, and their physical and spectral data are provided in the Supporting Information.

3.1.2. Crystal structure of Y₁₁

As shown in Fig. 3, the crystal structure of Y₁₁ was determined by single-crystal X-ray difference traction analysis. The skele-

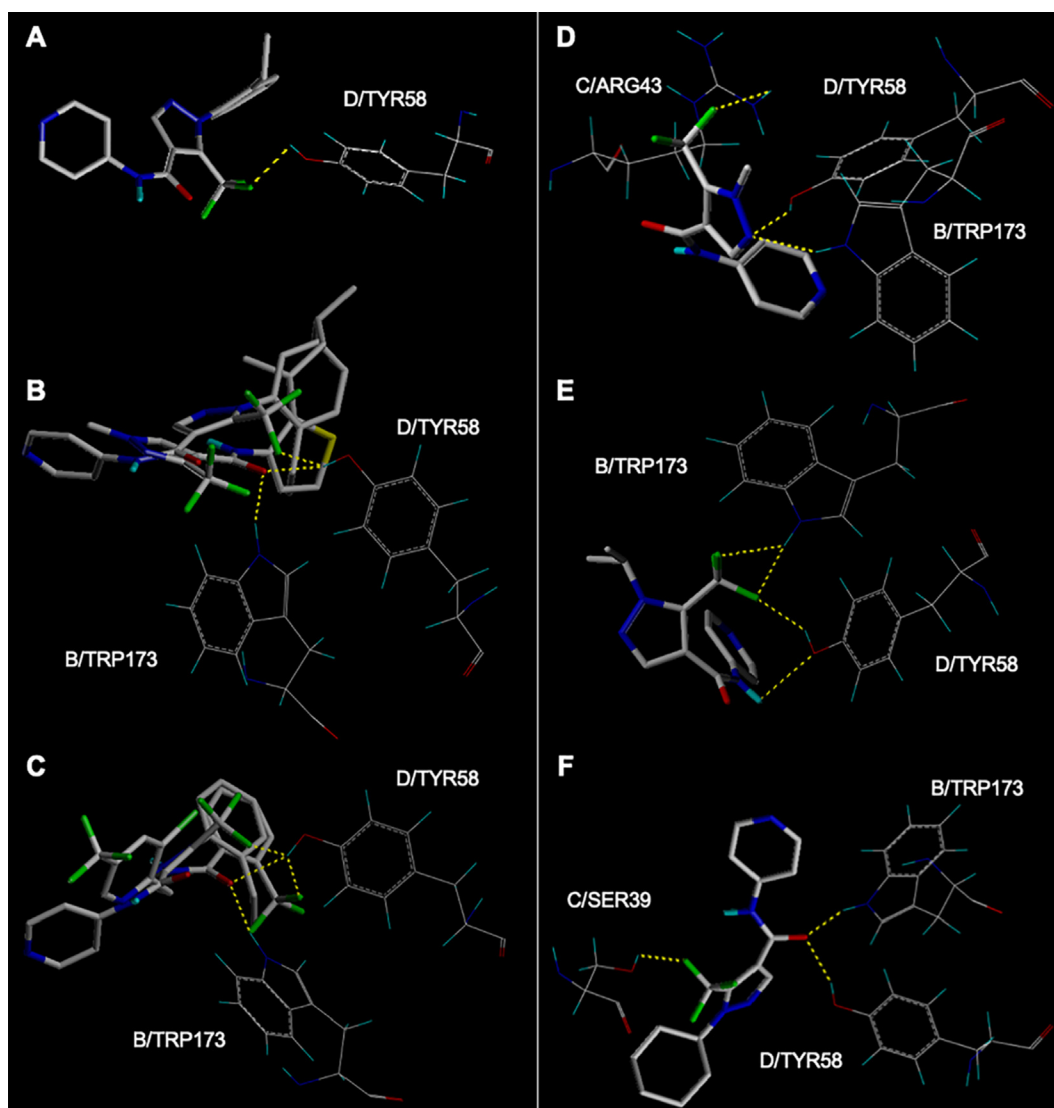


Fig. 4 Binding modes between ligands and SDH protein. (A) Y_{13} ; (B) Y_{13} and penthiopyrad; (C) Y_{13} and fluopyram; (D) Y_1 ; (E) Y_5 ; (F) Y_9 .

ton of Y_{11} was composed of a pyrazole ring and a pyridine ring connected by amide bonds C (9) and C (12). The benzene ring and the trifluoromethyl on the pyrazole ring were attached to N (1) and C (8), respectively, indicating that 2-Cl-benzyl was attached at the 1-position of the pyrazole and trifluoromethyl was attached at the 5-position of the pyrazole. The crystallographic data of Y_{11} have been deposited in the Cambridge Crystallographic Data Centre under deposition number 2,116,345 and can also be downloaded in the [Supporting Information](#).

3.2. Antifungal activity

3.2.1. *In vitro* antifungal activity

The preliminary *in vitro* antifungal activity results for the target compounds against seven types of pathogenic fungi are depicted in [Table 1](#). Some compounds exhibited excellent and broad-spectrum antifungal activities at a concentration

of 100 mg/L, such as Y_{13} , Y_{14} and Y_{17} . As shown by the EC_{50} values in [Table 2](#), Y_{13} showed good antifungal activities against *G. zeae* (13.1 mg/L), *B. dothidea* (14.4 mg/L), *F. proliferatum* (13.3 mg/L) and *F. oxysporum* (21.4 mg/L); Y_{14} exhibited good antifungal activities against *B. dothidea* (18.1 mg/L); and Y_{17} exhibited good antifungal activities against *G. zeae* (16.8 mg/L) and *B. dothidea* (13.9 mg/L). Analysis of the *in vitro* antifungal activities revealed that when the substituents in the 1-position of pyrazole were *ortho*-substituted phenyls, target compounds exhibited good antifungal activities, such as Y_{13} , Y_{14} and Y_{17} ; but lower activities were observed when methyl, isopropyl and cyclohexyl were introduced to the 1-position of the pyrazole ring, such as Y_1 to Y_{12} . However, when 4-pyridinyl was introduced into the amine part of the carboxamide group, such as in Y_{13} and Y_{17} , the antifungal activities were obviously better than those of other compounds.

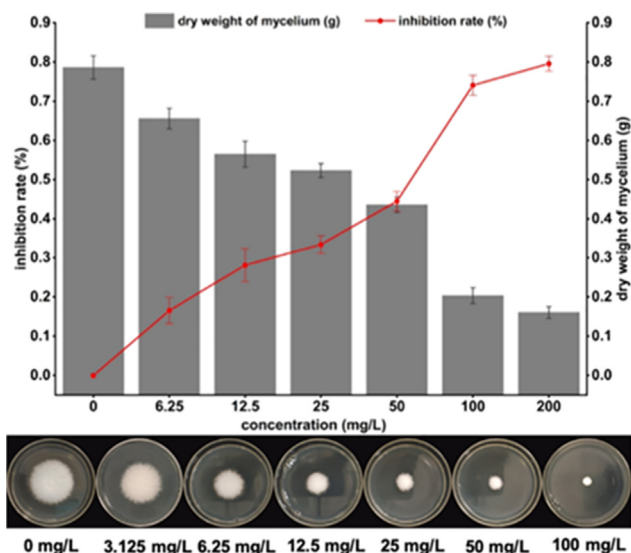


Fig. 5 Effects of Y₁₃ treatment on the growth of *G. zeae*.

3.2.2. *In vivo* antifungal activity of Y₁₃

Target compound Y₁₃ was selected for further *in vivo* antifungal activity evaluation against *G. zeae* on the leaves of maize. As shown in Table 3., Y₁₃ displayed obvious protective activity (50.65%) at 100 mg/L, which was lower than that of the commercialized fungicide phenamacril (79.83%). Further optimization of this series of target compounds containing *ortho*-substituted phenyl at the 1-position of pyrazole may lead to identification of compounds with higher activity that can be developed as potential fungicides against *G. zeae*.

3.3. SAR analysis

To further explore the SARs of the target compounds, reported SDH proteins (PDB: 2FBW, 3AEG and 7D6V) were used for docking studies. As shown by the docking results presented in Table 4, the total scores of ligands Y₃ and fluopyram docking to SDH protein (PDB: 2FBW) were 6.3 and 7.1, respectively, indicating that fluopyram exhibited a stronger interaction with 2FBW than Y₁₃. This is consistent with the activity results depicted in Tables 1 and 2. Through comparison of the interactions between Y₁₃ and the different SDH

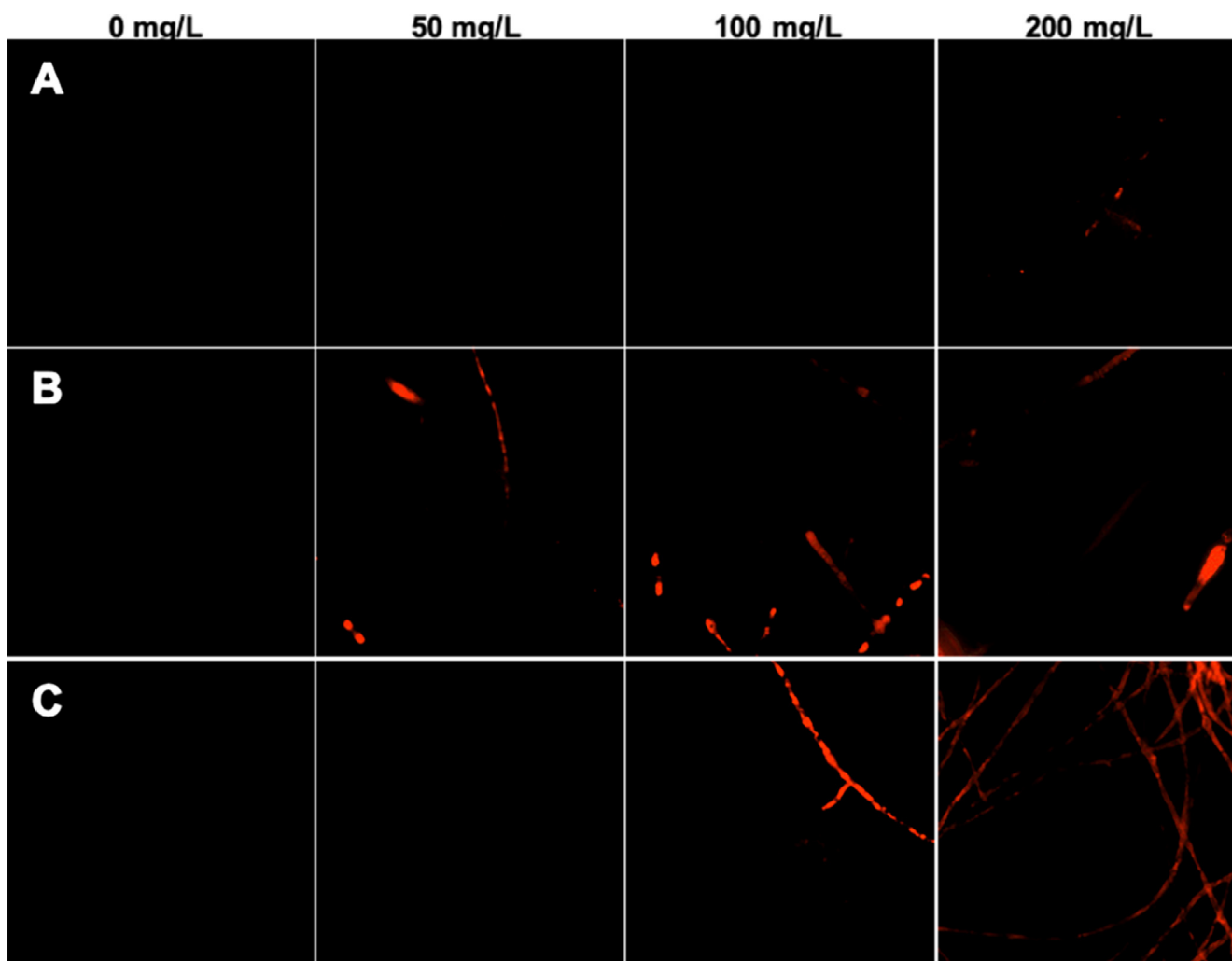


Fig. 6 Fluorescence observation of *G. zeae* treated with different compounds. A: Treatment with penthiopyrad at 0, 50, 100, and 200 mg/L; B: treatment with phenamacril at 0, 50, 100, and 200 mg/L; C: treatment with Y₁₃ at 0, 50, 100, and 200 mg/L.

proteins (2FBW, 3AEG and 7D6V), this binding model can be effectively evaluated for SAR analysis of this series of target compounds (Yan et al., 2021).

The docking results in Fig. 4A revealed that the trifluoromethyl group of Y_{13} formed a hydrogen bond with D/TYR58 (2.2 Å) of 2FBW. As shown in Fig. 4B, the oxygen atom of carbonyl in penthiopyrad formed hydrogen bonds with B/TRP173 (1.9 Å) and D/TYR58 (2.0 Å). Compared the binding modes of Y_{13} and penthiopyrad found that they bound tightly with 2FBW in the same pocket through roughly the similar conformation. As shown in Fig. 4C, the binding conformations of Y_{13} and fluopyram were similar, and the key group trifluoromethyl of two ligands both formed the hydrogen bonds with D/TYR58. The docking results demonstrated that the trifluoromethyl may be the key component of this series of molecules, contributing to the enhanced antifungal activity.

However, the docking poses and the docking scores were slightly changed when the substituent at the 1-position of the pyrazole ring was substituted. Compared the docking scores, binding modes (Fig. 4D, 4E and 4F) and antifungal activities of ligands Y_1 , Y_5 , and Y_9 found that when methyl, isopropyl and cyclohexyl were introduced at the 1-position of the pyrazole ring to replace the phenyl, the antifungal activities of the target compounds were decreased. Detailed analysis of the docking results for this series of target compounds revealed that Y_{13} exhibited better antifungal activity when phenyl was introduced to the 1-position of the pyrazole ring. These results were in agreement with the results of the preliminary SAR analysis. Thus, this molecular docking study may provide a benchmark for understanding the antifungal activity against plant phytopathogenic fungi *G. zeae*.

3.4. Effect of Y_{13} on mycelial growth of *G. Zeae*

As shown in Fig. 5, the dry weight of *G. zeae* hyphae treated with Y_{13} at different concentrations (0, 6.25, 12.5, 25, 50, 100, and 200 mg/L) for 24 h decreased significantly. Furthermore, the weight of hyphae decreased sharply as the concentration of Y_{13} increased, indicating that the target compound can inhibit the growth of *G. zeae* (Guo et al., 2020).

3.5. Effect of Y_{13} on the cell membrane integrity of *G. Zeae* mycelia

3.5.1. Morphological analysis via FM

PI, a nucleic acid dye that can enter through a disrupted cell membrane, stains upon binding to double-stranded nucleic acids (Li et al., 2020). The more and brighter the red fluorescence appears, the worse the cell membrane damage. As shown in Fig. 6, no fluorescence was observed in the CK groups (0 mg/L). As concentration increased, the fluorescence of hyphae treated with phenamacril (Fig. 6B) and Y_{13} (Fig. 6C) became stronger, which indicated that these compounds can destroy the integrity of the cell membrane and that the effects are concentration-dependent (Hou et al., 2021). However, the hyphae treated with penthiopyrad did not show obvious fluorescence, even at a concentration of 200 mg/L (Fig. 6A).

3.5.2. Morphological analysis via SEM

Morphological observation results for the hyphae of *G. zeae* treated with penthiopyrad, phenamacril, or Y_{13} at 200 mg/L are shown in Fig. 7. Compared with the hyphae treated with the different compounds, the normal hyphae presented regu-

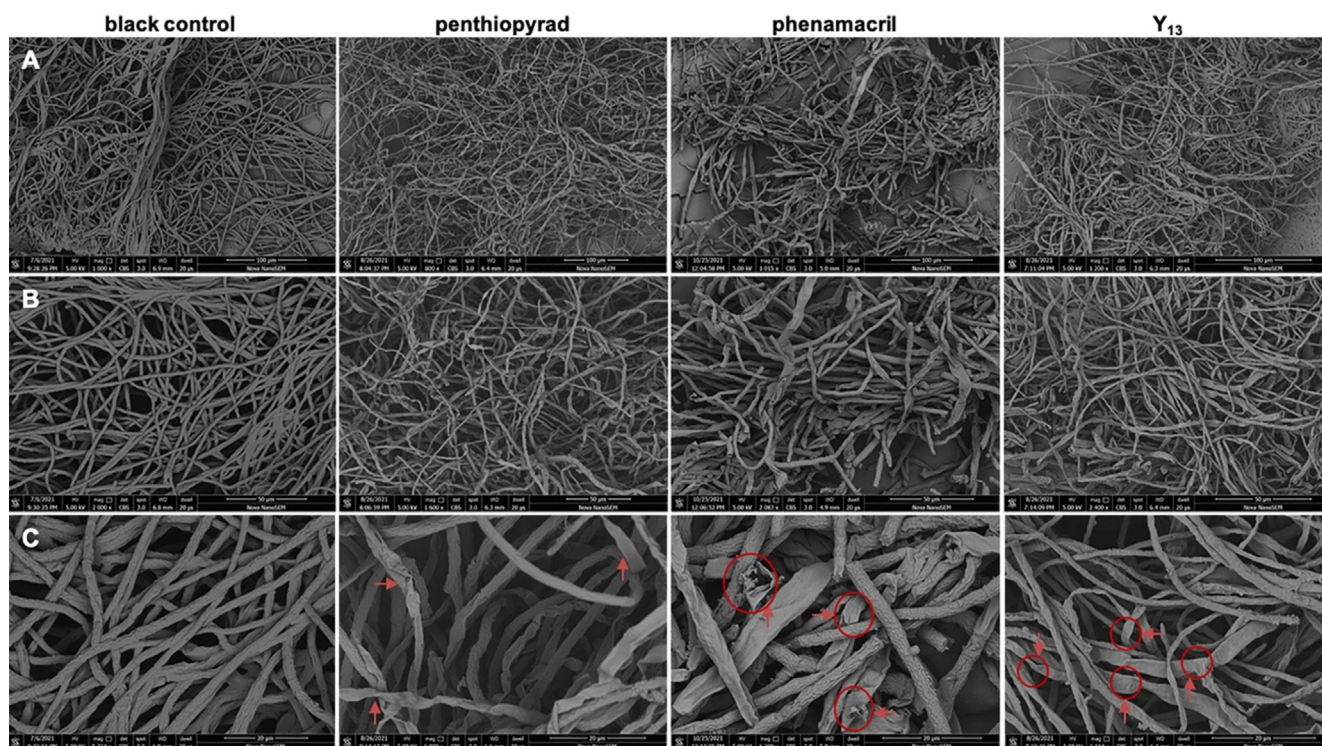


Fig. 7 SEM analysis: scanning electron micrographs of hyphae exposed to penthiopyrad phenamacril and Y_{13} at a concentration of 200 mg/L. A: 100 μ m. B: 50 μ m. C: 20 μ m. Arrows and arrowheads indicate hyphal shrinkage and partial distortion, respectively.

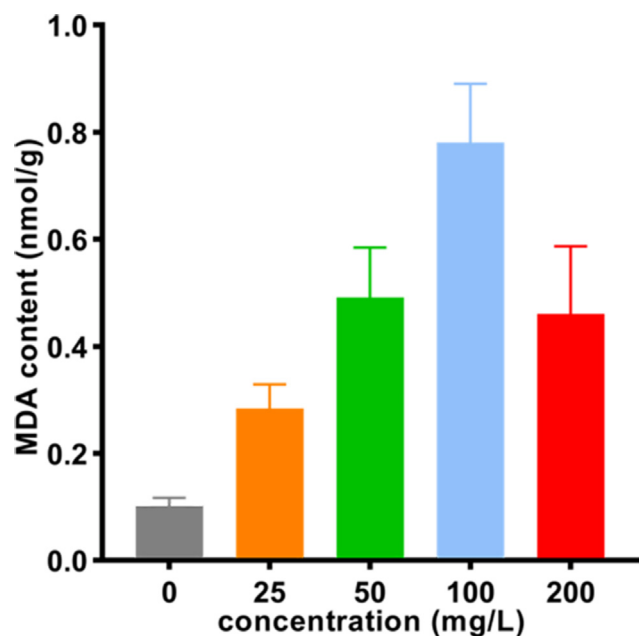


Fig. 8 MDA contents of *G. zoeae* treated with Y_{13} .

lar, smooth and uniform mycelia (blank control groups), and the hyphae treated with penthiopyrad exhibited a degree of shrinking (red arrows in Fig. 7C) but no breakage. However, the hyphae treated with phenamacril and Y_{13} showed obvious breakage, indicated by the red circles in Fig. 7C, which revealed that Y_{13} and phenamacril may disrupt the cell membrane of the mycelium, thus inhibiting the growth of the fungi (Zhao et al., 2020). This result was consistent with the findings of the FM morphological analysis described above.

3.6. MDA content of *G. Zeae* treated with Y_{13}

MDA, a sustainable biochemical marker, is produced in the process of lipid peroxidation, and the MDA content can be used to evaluate the degree of membrane damage (Zhao et al., 2016). The MDA contents of *G. zoeae* treated with Y_{13} at different concentrations (0, 25, 50, 100 and 200 mg/L) for 24 h are depicted in Fig. 8. The MDA content of *G. zoeae* mycelia increased when the concentration of Y_{13} increased (from 25 mg/L to 100 mg/L) and was obviously higher than the content in the control group (0 mg/L). However, when the concentration of Y_{13} was 200 mg/L, the MDA content decreased, indicating that a high concentration of Y_{13} can destroy the structure of the cell membrane and result in leakage of cell contents. All the results demonstrated that the target compound Y_{13} can promote lipid and peroxide reactions in cell membranes, which can lead to breakage of cell membranes (Yang et al., 2020).

The cells were treated for 24 h. The bars indicate the mean \pm SD ($n = 3$), and one-way ANOVA was used for statistical analysis among different groups. A significant difference was observed between the different treatment groups ($p < 0.05$).

4. Conclusion

A series of novel 1-substituted-5-trifluoromethyl-1*H*-pyrazole-4-carboxamide derivatives were designed and synthesized. In

in vitro bioassay results indicated that some target compounds exhibited excellent and broad-spectrum antifungal activities. Among them, the EC_{50} values of Y_{13} against *G. zoeae*, *B. dothidea*, *F. proliferatum* and *F. oxysporum* were 13.1, 14.4, 13.3, and 21.4 mg/L, respectively. Y_{13} also displayed certain protective activity (50.65%) against *G. zoeae* *in vivo* at 100 mg/L. SAR analysis revealed that the phenyl on the 1-position of the pyrazole ring was important for this activity. An antifungal mechanism study of Y_{13} against *G. zoeae* demonstrated that this compound may disrupt the cell membrane of mycelium, thus inhibiting the growth of fungi. These findings of the mechanistic studies were inconsistent with the findings for traditional amides and may provide a novel view for deep study of this series of pyrazole carboxamide derivatives.

Declaration of Competing Interest

The authors declare that they have no known competing financial interests or personal relationships that could have appeared to influence the work reported in this paper.

Acknowledgements

This work was supported by the National Natural Science Foundation of China (No. 32160655); and the Breeding Program of Guizhou University (No. 201931).

Appendix A. Supplementary material

Supplementary data to this article can be found online at <https://doi.org/10.1016/j.arabjc.2022.103987>.

References

- Abriegach, F., Bouchal, B., Riant, O., Mace, Y., Takfaoui, A., Radi, S., Oussaid, A., Bellaoui, M., Touzani, R., 2016. New *N, N, N', N'*-tetradentate pyrazoly agents: synthesis and evaluation of their antifungal and antibacterial activities. *J. Med. Chem.* 12 (1), 83–89.
- Al-Otibi, F., Perveen, K., Al-Saif, N.A., Alharbi, R.I., Bokhari, N.A., Albasher, G., Al-Otaibi, R.M., Al-Mosa, M.A., 2021. Biosynthesis of silver nanoparticles using *Malva parviflora* and their antifungal activity. *Saudi J. Biol. Sci.* 28 (4), 2229–2235.
- Chen, L., Huang, G.L., Lü, M.H., Zhang, Y.X., Xu, J., Bai, S.P., 2020. Amide derivatives of gallic acid: Design, synthesis and evaluation of inhibitory activities against *in vitro* α -synuclein aggregation. *Bioorg. Med. Chem.* 28, (15) 115596.
- Du, S.J., Li, Z.H., Tian, Z.M., Xu, L., 2018. Synthesis, antifungal activity and QSAR of novel pyrazole amides as succinate dehydrogenase inhibitors. *Heterocycles* 96, 74–85.
- Fu, L., Chen, Y., Guo, H., Xu, L., Tan, M., Dong, Y., Shu, M., Wang, R., Lin, Z., 2021. A selectivity study of polysubstituted pyridinylimidazoles as dual inhibitors of JNK3 and p38 α MAPK based on 3D-QSAR, molecular docking, and molecular dynamics simulation. *Struct. Chem.* 32 (2), 819–834.
- Gonzalez-Lopez, E., Leon-Jaramillo, J., Trilleras, J., Grande-Tovar, C.D., Peralta-Ruiz, Y., Quiroga, J., 2020. Synthesis and evaluation of the fungal activity of new pyrazole-carboxamides against *Colletotrichum gloeosporioides*. *J. Braz. Chem. Soc.* 31 (9), 1917–1925.
- Guo, Y.T., Lv, J., Zhao, Q., Dong, Y., Dong, K., 2020. Cinnamic acid increased the incidence of *Fusarium* wilt by increasing the pathogenicity of *Fusarium oxysporum* and reducing the physiolog-

- ical and biochemical resistance of faba bean, which was alleviated by intercropping with wheat. *Front. Plant Sci.* 11, 608389.
- Hua, X.W., Liu, W.R., Su, Y.Y., Liu, X.H., Liu, J.B., Liu, N.N., Wang, G.Q., Jiao, X.Q., Fan, X.Y., Xue, C.M., Liu, Y., Liu, M., 2020. Studies on the novel pyridine sulfide containing SDH based heterocyclic amide fungicide. *Pest Manag. Sci.* 76 (7), 2368–2378.
- Hou, S.T., Xie, D.W., Yang, J.X., Niu, X., Hu, D.Y., Wu, Z.B., 2021. Design, synthesis and antifungal evaluation of novel mandelic acid derivatives containing a 1,3,4-oxadiazothioether moiety. *Chem. Biol. Drug Des.* 98 (1), 166–174.
- Jian, W.L., He, D.H., Song, S.Y., 2016. Synthesis, biological evaluation, and molecular modeling studies of new oxadiazole-stilbene hybrids against phytopathogenic fungi. *Sci. Rep.* 6, 31045.
- Kaddouri, Y., Abridgach, F., Ouahhoud, S., Benabbes, R., Kodadi, M. E., Alsalmeh, A., Al-Zaqri, N., Warad, I., Touzani, R., 2021. Synthesis, characterization, reaction mechanism prediction and biological study of mono, bis and tetrakis pyrazole derivatives against *Fusarium oxysporum f. sp. Albedinis* with conceptual DFT and ligand-protein docking studies. *Bioorg. Chem.* 110, 104696.
- Kaddouri, Y., Abridgach, F., Ouahhoud, S., Benabbes, R., Kodadi, M. E., Alsalmeh, A., Al-Zaqri, N., Warad, I., Touzani, R., 2020. Mono-Alkylated ligands based on pyrazole and triazole derivatives tested against *Fusarium oxysporum f. sp. Albedinis*: Synthesis, characterization, DFT, and phytase binding site identification using blind docking/virtual screening for potent fophy inhibitors. *Front. Chem.* 1073.
- Kim, C., Kim, J., Park, H.Y., Lee, J.H., Park, H.J., Kim, C.K., Yoon, J., 2009. Structural understanding of quorum-sensing inhibitors by molecular modeling study in *Pseudomonas aeruginosa*. *Appl. Microbiol. Biotechnol.* 83 (6), 1095–1103.
- Kim, C., Kim, J., Park, H.Y., Park, H.J., Kim, C.K., Yoon, J., Lee, J. H., 2009. Development of inhibitors against TraR quorum-sensing system in *Agrobacterium tumefaciens* by molecular modeling of the ligand-receptor interaction. *Mol. Cells* 28 (5), 447–453.
- Komane, P.P., Kumar, P., Choonara, Y.E., Pillay, V., 2020. Functionalized, vertically super-aligned multiwalled carbon nanotubes for potential biomedical applications. *Int. J. Mol. Sci.* 21 (7), 2276.
- Ke, Y., Ding, B.B., Zhang, M.M., Dong, T.J., Fu, Y., Lv, Q.Y., Ding, W.P., Wang, X.D., 2022. Study on inhibitory activity and mechanism of chitosan oligosaccharides on *Aspergillus Flavus* and *Aspergillus Fumigatus*. *Carbohydr. Polym.* 275, 118673.
- Liu, K., Shang, X.Y., Cheng, Y.Y., Chang, X.Y., Li, P.F., Li, W.J., 2018. Regioselective [3 + 2]-annulation of hydrazonyl chlorides with 1,3-dicarbonyl compounds for assembling of polysubstituted pyrazoles. *Org. Biomol. Chem.* 16 (42), 7811–7814.
- Liu, X.H., Qiao, L., Zhai, Z.W., Cai, P.P., Cantrell, C.L., Tan, C.X., Weng, J.Q., Han, L., Wu, H.K., 2019. Novel 4-pyrazole carboxamide derivatives containing flexible chain motif: design, synthesis and antifungal activity. *Pest Manag. Sci.* 75 (11), 2892–2900.
- Luo, D.X., Guo, S.X., He, F., Wang, H.Y., Xu, F.Z., Dai, A.L., Zhang, R.F., Wu, J., 2020. Novel anthranilic amide derivatives bearing the chiral thioether and trifluoromethylpyridine: Synthesis and bioactivity. *Bioorg. Med. Chem. Lett.* 30, (3) 126902.
- Li, J.L., Islam, S., Guo, P.F., Hu, X.Q., Dong, W.B., 2020. Isolation of antimicrobial genes from *Oryza rufipogon* griffby using a *Bacillus subtilis* expression system with potential antimicrobial activities. *Int. J. Mol. Sci.* 21 (22), 8722.
- McColl, A.I., Bleackley, M.R., Anderson, M.A., Lowe, R., 2018. Resistance to the plant defensin NaDI features modifications to the cell wall and osmo-regulation pathways of yeast. *Front. Microbiol.* 9, 1648.
- Mo, F.X., Hu, X.F., Ding, Y., Li, R.Y., Long, Y.H., Wu, X.M., Li, M., 2021. Naturally produced magnolol can significantly damage the plasma membrane of *Rhizoctonia solani*. *Pestic. Biochem. Physiol.* 178, 104942.
- Ninomiya, A., Urayama, S.I., Suo, R., Itoi, S., Fuji, S.I., Moriyama, H., Hagiwara, D., 2020. Mycovirus-induced tenuazonic acid production in a rice blast fungus *Magnaporthe oryzae*. *Front. Microbiol.* 11, 1641.
- Oporto, C.I., Villarreal, C.A., Tapia, S.M., García, V., Cubillos, F.A., 2019. Distinct transcriptional changes in response to patulin underlie toxin biosorption differences in *Saccharomyces cerevisiae*. *Toxins (Basel)*. 11 (7), 400.
- Wang, H., Ren, S.X., He, Z.Y., Wang, D.L., Yan, X.N., Feng, J.T., Zhang, X., 2014. Synthesis, antifungal activities and qualitative structure activity relationship of carbonyl hydrazone derivatives as potential antifungal agents. *Int. J. Mol. Sci.* 15 (3), 4257–4272.
- Wang, D.W., Zhang, R.B., Yu, S.Y., Liang, L., Ismail, I., Li, Y.H., Xu, H., Wen, X., Xi, Z., 2019. Discovery of novel *N*-isoxazolinyphenyltriazinones as promising protoporphyrinogen IX oxidase inhibitors. *J. Agric. Food Chem.* 67 (45), 12382–12392.
- Wang, X.B., Wang, A., Qiu, L.L., Chen, M., Lu, A.M., Li, G.H., Yang, C.L., Xue, W., 2020. Expedient discovery for novel antifungal leads targeting succinate dehydrogenase: Pyrazole-4-formylhydrazone derivatives bearing a diphenyl ether fragment. *J. Agric. Food Chem.* 68 (49), 14426–14437.
- Wang, Q.Q., Zhang, S.G., Jiao, J., Dai, P., Zhang, W.H., 2021. Novel fluorinated 7-hydroxycoumarin derivatives containing an oxime ether moiety: design, synthesis, crystal structure and biological evaluation. *Molecules* 26 (2), 372.
- Wu, Z.B., Park, H.Y., Xie, D.W., Yang, J.X., Hou, S.T., Shahzad, N., Kim, C.K., Yang, S., 2021. Synthesis, biological evaluation, and 3D-QSAR studies of *N*-(Substituted pyridine-4-yl)-1-(substituted phenyl)-5-trifluoromethyl-1*H*-pyrazole-4-carboxamide derivatives as potential succinate dehydrogenase inhibitors. *J. Agric. Food Chem.* 69 (4), 1214–1223.
- Wang, W., Wang, J.H., Wu, F.R., Zhou, H., Xu, D., Xu, G., 2021. Synthesis and biological activity of novel pyrazol-5-yl-benzamide derivatives as potential succinate dehydrogenase inhibitors. *J. Agric. Food Chem.* 69 (20), 5746–5754.
- Xiong, Z.Q., Tu, X.R., Wei, S.J., Huang, L., Li, X.H., Lu, H., Tu, G. Q., 2013. *In vitro* antifungal activity of antifungalmycin 702, a new polyene macrolide antibiotic, against the rice blast fungus *Magnaporthe grisea*. *Biotechnol. Lett.* 35 (9), 1475–1479.
- Xiong, L., Li, H., Jiang, L.N., Ge, J.M., Yang, W.C., Zhu, X.L., Yang, G.F., 2017. Structure-based discovery of potential fungicides as succinate ubiquinone oxidoreductase inhibitors. *J. Agric. Food Chem.* 65 (5), 1021–1029.
- Yan, C., Dong, J., Liu, Y., Li, Y., Wang, Q., 2021. Target-directed design, synthesis, antiviral activity, and SARs of 9-substituted phenanthroindolizidine alkaloid derivatives. *J. Agric. Food Chem.* 69 (27), 7565–7571.
- Yan, W., Wang, X., Li, K., Li, T.X., Wang, J.J., Yao, K.C., Cao, L.L., Zhao, S.S., Ye, Y.H., 2019. Design, synthesis, and antifungal activity of carboxamide derivatives possessing 1,2,3-triazole as potential succinate dehydrogenase inhibitors. *Pestic. Biochem. Physiol.* 156, 160–169.
- Yang, D.Y., Zhao, B., Fan, Z.J., Yu, B., Zhang, N.L., Li, Z.M., Zhu, Y.L., Zhou, J.H., Kalinina, T.A., Glukhareva, T.V., 2019. Synthesis and biological activity of novel succinate dehydrogenase inhibitor derivatives as potent fungicide candidates. *J. Agric. Food Chem.* 67 (47), 13185–13194.
- Yang, Q., Wang, J., Zhang, P., Xie, S.N., Yuan, X.L., Hou, X.D., Yan, N., Fang, Y.D., Du, Y.M., 2020. *In vitro* and *in vivo* antifungal activity and preliminary mechanism of cembratrien-diols against *Botrytis cinerea*. *Ind. Crops Prod.* 154, 112745.
- Zhang, X.X., Jin, H., Deng, Y.J., Gao, X.H., Li, Y., Zhao, Y.T., Tao, K., Hou, T.P., 2017. Synthesis and biological evaluation of novel pyrazole carboxamide with diarylamine-modified scaffold as potent antifungal agents. *Chin. Chem. Lett.* 28 (8), 1731–1736.
- Zhang, A.G., Yue, Y., Yang, Y.H., Yang, J., Tao, K., Jin, H., Hou, T. P., 2019. Discovery of *N*-(4-fluoro-2-(phenylamino)phenyl)-pyrazole-4-carboxamides as potential succinate dehydrogenase inhibitors. *Pestic. Biochem. Physiol.* 158, 175–184.

- Zhao, Y.L., Wang, Y.K., Yang, H., Wang, W., Wu, J.Y., Hu, X.L., 2016. Quantitative proteomic analyses identify ABA-Related proteins and signal pathways in maize leaves under drought conditions. *Front. Plant Sci.* 7, 1827.
- Zhao, Y.T., Yang, N., Deng, Y.M., Tao, K., Jin, H., Hou, T.P., 2020. Mechanism of action of novel pyrazole carboxamide containing a diarylamine scaffold against *Rhizoctonia solani*. *J. Agric. Food Chem.* 68 (40), 11068–11076.
- Zhu, N., Jin, H.M., Kong, X.P., Zhu, Y.Y., Ye, X.M., Xi, Y.L., Du, J., Li, B.Q., Lou, M.H., Shah, G.M., 2020. Improving the fermentable sugar yields of wheat straw by high-temperature pre-hydrolysis with thermophilic enzymes of *Malbranchea cinnamomea*. *Microb. Cell Fact.* 19 (1), 149.